Computation of Flows in a Turn-Around Duct and a Turbine Cascade Using Advanced Turbulence Models

B. Lakshminarayana and J. Luo
Department of Aerospace Engineering
The Pennsylvania State University
University Park, PA 16802

Summary

Numerical investigation has been carried out to evaluate the capability of the Algebraic Reynolds Stress Model (ARSM) and the Nonlinear Stress Model (NLSM) to predict strongly curved turbulent flow in a turn-around duct (TAD). The ARSM includes the near-wall damping term of pressure-strain correlation ($\phi_{ij,w}$), which enables accurate prediction of individual Reynolds stress components in wall flows. The TAD mean flow quantities are reasonably well predicted by various turbulence models. The ARSM yields better predictions for both the mean flow and the turbulence quantities than the NLSM and the k-ε (k=turbulent kinetic energy, ε=dissipation rate of k) model. The NLSM also shows slight improvement over the k-ε model. However, all the models fail to capture the recovery of the flow from strong curvature effects. The formulation for $\phi_{ij,w}$ appears to be incorrect near the concave surface.

The hybrid k-ε/ARSM, Chien's k-ε model and Coakley's q-ω ($q = \sqrt{k}$, $\omega = \varepsilon/k$) model have also been employed to compute the aerodynamics and heat transfer of a transonic turbine cascade. The surface pressure distributions and the wake profiles are predicted well by all the models. The k-ε model and the k-ε/ARSM model provide better predictions of heat transfer than the q-ω model. The k-ε/ARSM solutions show significant differences in the predicted skin friction coefficients, heat transfer rates and the cascade performance parameters, as compared to the k-ε model. The k-ε/ARSM model appears to capture, qualitatively, the anisotropy associated with by-pass transition.

Numerical Technique

An explicit two-dimensional Navier-Stokes solver -- RK2D (Kunz & Lakshminarayana, 1992) was used in the computation. The RK2D uses a standard 4-stage Runge-Kutta scheme. The fourth-order artificial dissipation is included to damp high wave number errors and the second-order artificial dissipation is used to improve the shock capturing. Anisotropic scaling of artificial dissipation terms was used. By the use of local velocity scaling, the smoothing was reduced to zero near the wall to avoid contamination of the solution by excessive dissipation. Local variable timestepping was also used to improve convergence. In the near wall viscous sublayer and buffer layer, the low Reynolds number k-ε model is used. The matching point for ARSM (or NLSM) and k-ε model is at $y^+ = 50$ ($y^+ = yu_\tau/\nu$, y=distance from the wall, u_τ=friction velocity, ν=kinematic viscosity).

Results and Discussion

1) Computation and Analysis of the Flow in a Turn-Around Duct

Most rocket engine components operate at very high pressures and Reynolds numbers and the flows are fully turbulent. These flows are often subjected to very large strain-rates such as those arising from the strong streamline curvature. There have been many studies on the effects of streamline curvature, however, most deal with mild curvature. Bradshaw (1973) reviewed the literature prior to 1973. Recently, Monson et al. (1990) reported detailed measurements in a two-dimensional TAD air tunnel at Mach no.=0.1 and $Re=10^5$ or $Re=10^6$. They also calculated this TAD flow using several different versions of k-ε models and found that only one extended model gave reasonable predictions. The present investigation has been carried out with more advanced turbulence models, namely, the ARSM, which was derived from Gibson & Launder (1978) Reynolds Stress Model (RSM) by invoking the ARSM assumption, and the NLSM of Shih et al. (1992). A 201x101 (streamwise x normal direction) H-grid is generated by algebraic method.

The k-ε/ARSM model was validated against a flat plate boundary layer. The computed values of turbulence intensities are in good agreement with Klebanoff's data (1954) for a flat plate boundary layer, as shown in Fig. 1. For the TAD flow, all the three turbulence models predict the static pressure coefficients very well on both the inner and the outer walls along the bend, as can be seen in the Fig. 2. The pressure loss and static pressure downstream of the bend are also predicted reasonably well by all the three models. However, the NLSM predicts a larger separation region on the inner wall than the measurement, which can be seen from the underprediction of the pressure coefficient near the exit of the bend.

Fig. 3(a) shows longitudinal velocity profiles predicted by the k-ε model (with Chien's near wall function slightly modified), NLSM and ARSM models. All the models underpredict the velocity near the outer wall. However, the turbulent kinetic energy (TKE) and turbulent shear stress (TSS) profiles are predicted reasonably well by all the models. As shown in Fig. 3(b) and 3(c), the reduction of turbulent shear stress near the convex (inner) wall is predicted well. The predicted enhancement of turbulence near the concave (outer) wall is in agreement with the experiment (Fig. 3(c)). As shown in the figures, prediction of turbulence quantities from the ARSM is consistently better than those from the NLSM and k-ε models.

At the exit of the bend (θ=180 deg), the data indicate that the flow is separated on the convex wall (Fig. 4(a)). All the models predict separation, but underpredict the height of the separation bubble. The prediction of mean velocity by the ARSM is slightly better than those from the NLSM and the k-ε models. The TKE level near the mid-channel was underpredicted significantly by all the models (Fig. 4(b)), this is due to underprediction of the radial component of normal stresses near the outer wall. It could be due to the breakdown of the ARSM assumption, i.e., the $\overline{u_i u_j}/k$ is constant in the flowfield, or the deficiency of the present formulation for the pressure-strain correlation and the dissipation rate of k (i.e., ε).

2) Computation of the transonic turbine cascade flow

The aerodynamics and blade heat transfer data of the VKI transonic linear turbine guide vane cascade measured by Arts, et al. (1990) was selected as the primary test case for present work. The turbine blade shape tested was optimized for a downstream isentropic Mach number of 0.9. The downstream isentropic Reynolds number (based on chord length) varied from 0.6×10^6 to 2.1×10^6. The total temperature in the free stream was around $410(^0k)$ and the blade surface temperature was constant at about $300(^0k)$ for all the test runs. The freestream turbulence intensity varied from 1% to 6%. The inlet flow

angle was β_1=0 (deg), chord length C=67.65 (mm), pitch/chord=0.85, stagger angle=55 (deg), axial chord length C_{ax}=37.0 (mm), design outlet angle β_2=74 (deg). For numerical details, see Luo & Lakshminarayana (1993).

A 129x71 H-grid is used. Blade surface pressure distributions, blade wake, aerodynamic losses and exit flow angles are captured very well by all the three models. The blade isentropic Mach no., including the effect of shock wave, is captured accurately by all the models, as shown in Fig. 5. Fig. 6 shows the comparison of computed and measured wake profiles. The agreement is very good from all the three models. The semi-wake width is shown in Fig. 7. Sudden increase in wake width at downstream locations A and B is attributed to shock/wake interaction. It is clear that the correlation shown in Fig. 7 is not valid when shock waves are present at the cascade exit. Except for the shock/wake interaction region the wake width follows the correlation. In Fig. 8, the predictions of heat transfer by all the models are shown and these are in good agreement with the data. The transition is triggered by the shock wave and this has been captured by all the models. The boundary layer code (TEXSTAN) underpredicts the heat transfer on the pressure surface and the solution is terminated on the suction surface near the inception of separation. Sharma et al. (1982) have observed that most of the disturbance energy is contained in the streamwise component of turbulence intensity before transition. During the transition, both the streamwise and the normal components grow with the latter component growing at a faster rate than the former, resulting in a decrease of the relative magnitude of the streamwise intensity . As can be seen from Fig. 9, this evolution of streamwise and normal turbulence intensity within the boundary layer during transition appears to have been simulated qualitatively by the k-ε/ARSM model.

Acknowledgements

This work was supported by the NASA through contract NAS 8-38867 monitored by Lisa Griffin of Marshall Space Flight Center, and by the Penn State - NASA Propulsion Center. The authors wish to acknowledge NASA for providing the supercomputing resoures at NASA Lewis and Marshall Research Centers.

References

Arts, T., Rouvroit, M. L. and Rutherford, A. W., 1990, "Aero-thermo Investigation of a Highly Loaded Transonic Linear Turbine Guide Vane Cascade," Von Karman Institute TN 174. Also, *Journal of Turbomachinery*, Vol. 114, pp. 147-154.

Bradshaw, P., 1973, "Effects of Streamline Curvature on Turbulent Flow," *AGARD-AG-169*.

Chien, K. Y., 1982, "Prediction of Channel and Boundary-Layer Flows with a Low-Reynolds Number Turbulence Model," *AIAA Journal*, Vol. 20, No. 1.

Coakley, T.J., 1983, "Turbulence Modeling Methods for the Compressible Navier-Stokes Equations", *AIAA Paper 83-1693*.

Gibson, M. and Launder, B., 1978, "Ground Effects on Pressure Fluctuations in the Atmospheric Boundary Layer," *J. Fluid Mech.*,vol. 86, pp.491.

Klebanoff, P., 1954, "Characteristics of Turbulence in a Boundary Layer with Zero Pressure Gradient," *NACA TN-3178*.

Kunz, R. and Lakshminarayana, B., 1992, "Explicit Navier-Stokes Computation of Cascade Flows Using the k-ε Model," *AIAA Journal*, Vol. 30, No. 1.

Luo, J. and Lakshminarayana, B., 1993, "Navier-Stokes Analysis of Turbine Aerodynamics and External Heat Transfer," *ISABE paper*, Tokyo.

Monson, D. J., Seegmiller, H.L. , McConnaughey, P. K. and Chen, Y. S., 1990, "Comparison of Experiment with Calculations Using Curvature-Corrected Zero and Two Equation Turbulence Models for a Two-Dimensional U-Duct," *AIAA paper 90-1484*.

Sharma, O. P., Wells, R. A., Schlinker, R. H. and Bailey, D. A., 1982,"Boundary Layer Development on Turbine Airfoil Suction Surfaces," *Journal of Engineering for Power*, Vol. 104, pp. 698-706.

Shih, T., Zhu, J. and Lumley, J. L., 1992, "A Realizable Reynolds Stress Algebraic Equation Model," *NASA TM 105993*.

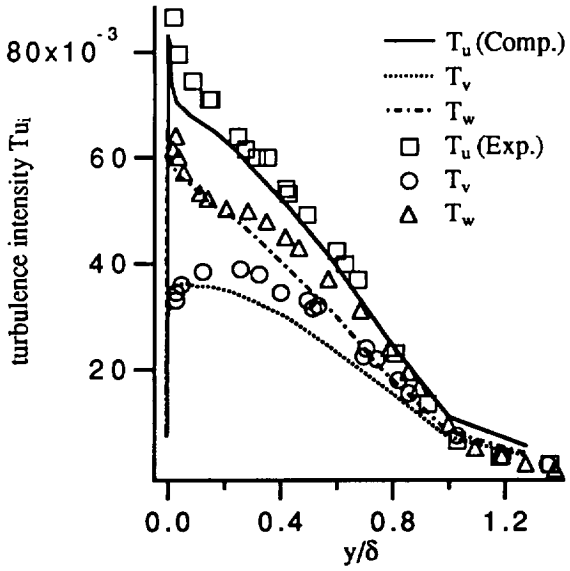

Fig. 1 Turbulence intensity profiles in the flat-plate turbulent boundary layer: experiment by Klebanoff; computation by 2-layer k-ε/ARSM; y=normal distance to the wall, δ=boundary layer thickness, Tu_i=turbulence intensity components.

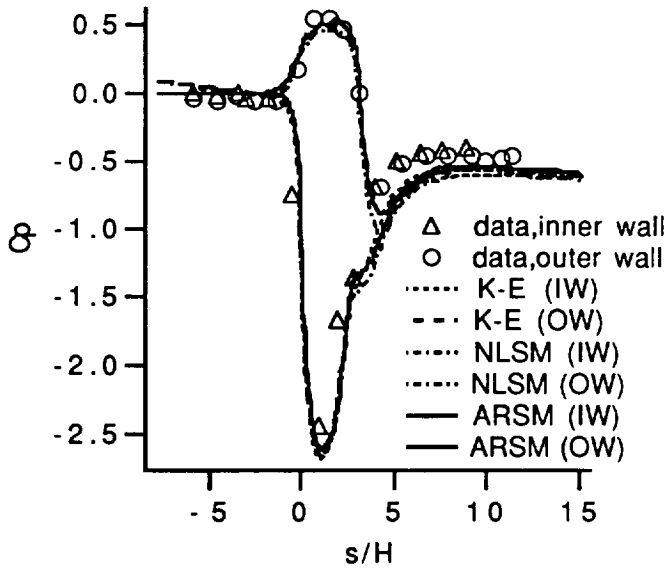

Fig. 2 Static pressure coefficient (C_p) on turn-around duct inner and outer walls; S=streamwise distance, H=duct height, $C_p=(P-P_{ref})/(1/2\rho U_m^2)$, P_{ref}=static pressure at inlet, U_m=bulk velocity

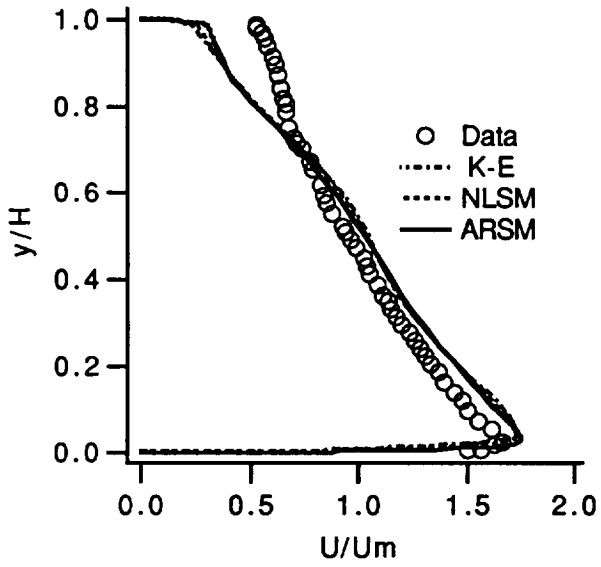

Fig. 3(a) Longitudinal velocity (U) in turn-around duct, θ=90 deg.; U_m=bulk velocity, θ=angle into bend, y=normal distance to the inner wall.

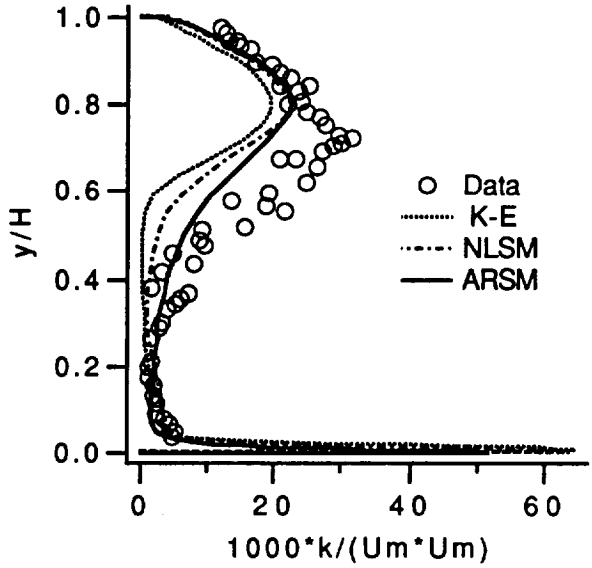

Fig. 3(b) Turbulent kinetic energy (k) profile

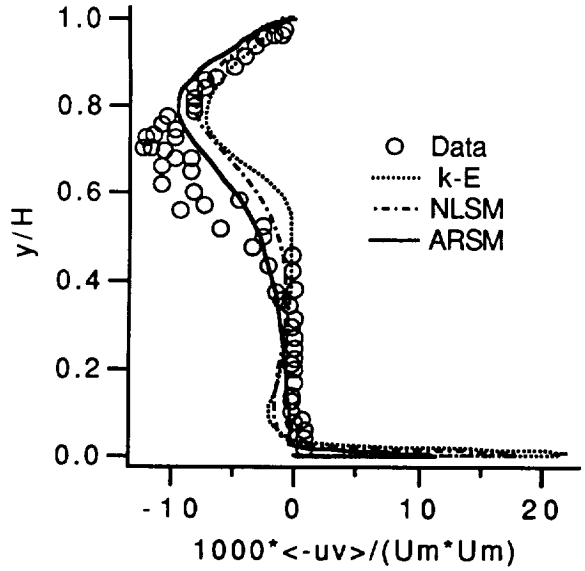

Fig. 3(c) Turbulent shear stress (<-uv>) profile

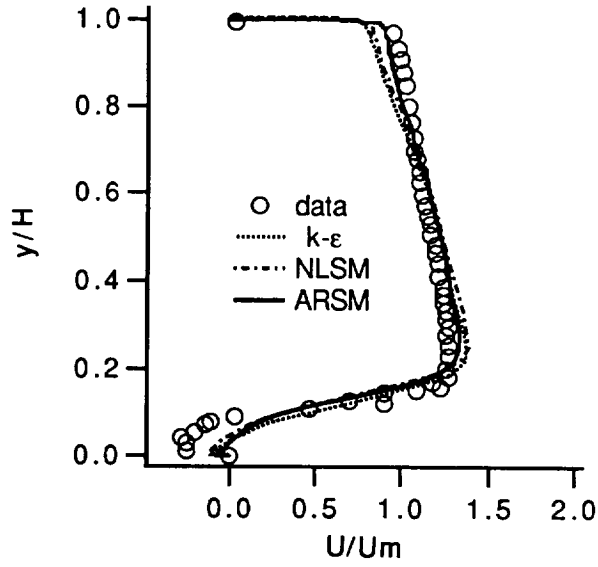

Fig. 4(a) Longitudinal velocity in turn-around duct, θ = 180 deg

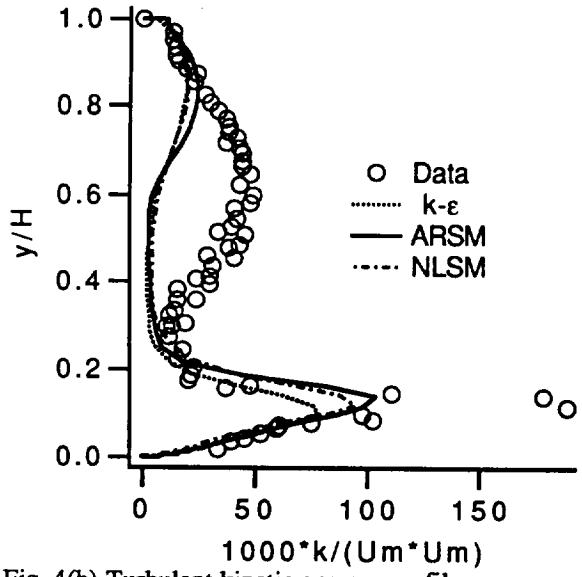

Fig. 4(b) Turbulent kinetic energy profile

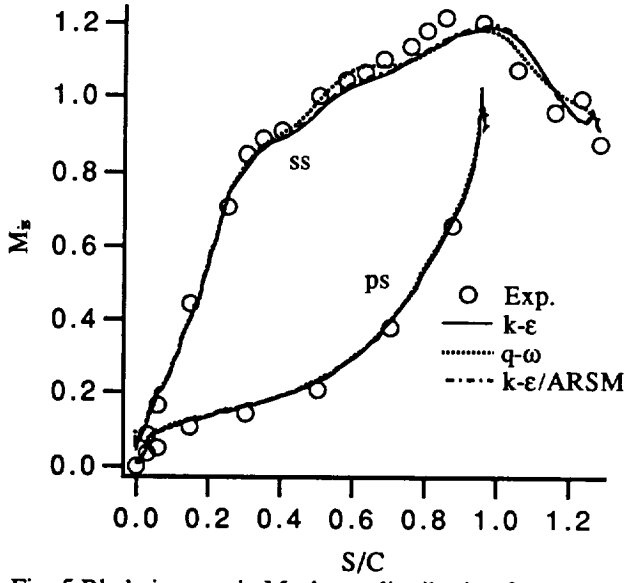

Fig. 5 Blade isentropic Mach no. distribution for case Mur049 ($M_{is,2}$=1.02,$Re_{is,2}$=1.0x10^6 and Tu_∞=1%); S = coordinate along blade surface, C = chord length, ss = suction surface, ps = pressure surface.

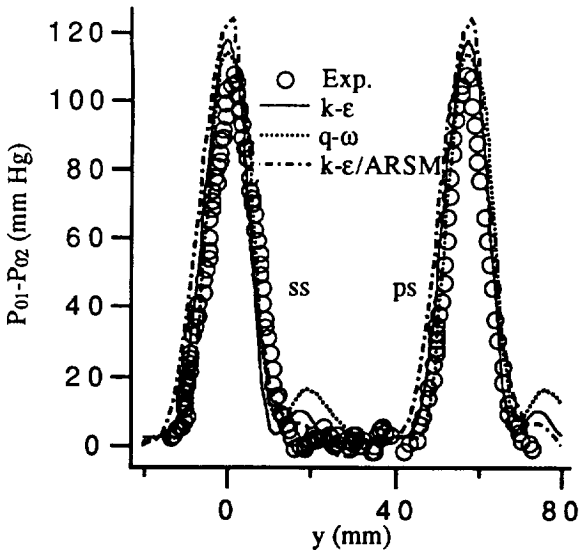

Fig. 6 Computed and measured wakes at x/C_{ax} =1.433 for the above case; P_{01}-P_{02}=total pressure loss, x=coordinate along axial chord, y=pitchwise coordinate, C_{ax}=axial chord length

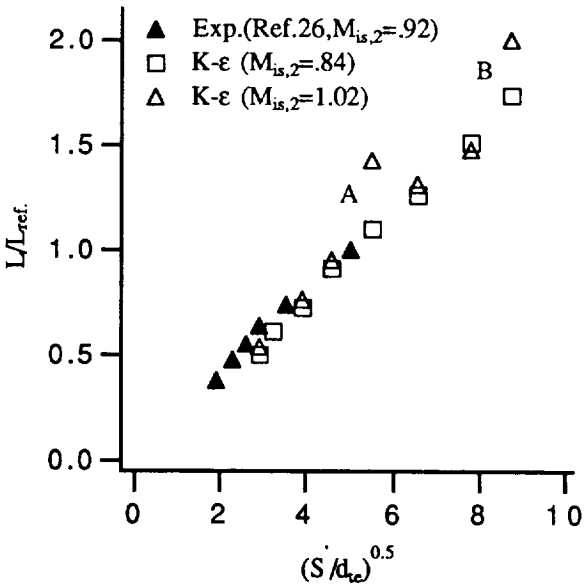

Fig. 7 Wake width growth downstream of the blade. L=semi-wake width, S'/d_{te}=non-dimensional distance in exit flow direction

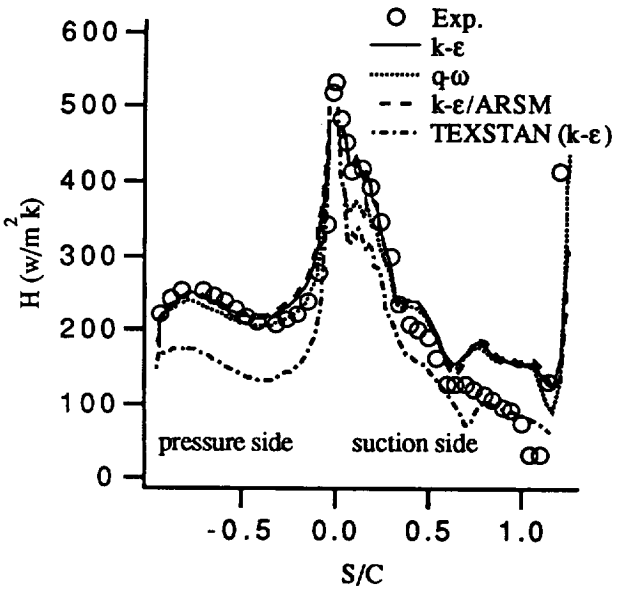

Fig. 8 Heat transfer prediction for case Mur222 ($M_{is,2}$= 1.14, $Re_{is,2}$=0.55x10^6 and Tu_∞=6%); H=heat transfer coefficient.

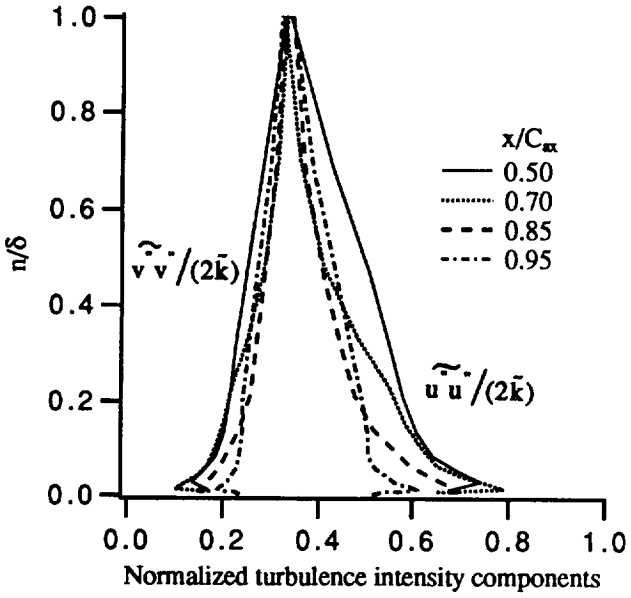

Fig. 9 The normalized turbulence intensity component profiles (Computed by k-ε/ARSM) at different axial chordwise locations on the suction surface (n is the normal distance to the wall and δ is the boundary layer thickness)